Parameterising Heat Diffusion Equations in 2D/3D Geometries

Luke Filippini

Supervised by Dr Elliot Carr

Queensland University of Technology

Contents

1 Abstract

The laser flash method is the most popular technique for estimating the thermal diffusivity of a material. It involves subjecting the front surface of a small sample of a material to a heat pulse of radiant energy for a short duration, then measuring the corresponding rear-surface temperature rise over time. In 2019, Carr and Wood proposed a model for a one-dimensional sample that incorporated a finite pulse time effect, using the rear-surface integral method to estimate the thermal diffusivity. This report presents an extension to this previous work, considering radial heat flow in two-dimensional annular geometries and three-dimensional spherical shell geometries. New formulas are derived and verified using synthetic data. Additionally, their sensitivity to three fixed levels of measurement noise are investigated. Lastly, the consideration of two-layer samples and varying levels of noise are identified as extensions for future work.

2 Introduction

Thermal diffusivity is a physical property of key importance in many industries. From insulating homes to reducing heat build-up in electrical equipment, optimal thermal inertia is desired for both functionality and safety. Knowledge of the *thermal diffusivity*, or the heat-conductive ability of a material relative to its storage capacity, is, therefore, vital to satisfy such a requirement. It is, therefore, unsurprising that we find such a property as an integral part of the heat diffusion equation (Salazar, 2003).

The heat diffusion equation describes the spreading out of heat to regions that are cooler, relatively speaking, than areas where heat is concentrated. Hence, such a model is essential for describing and understanding thermodynamic systems. At any given point, when heat is flowing in or out of a material, the increase, or decrease, in temperature is proportional to the the thermal diffusivity. Typically, the thermal diffusivity is defined as the constant α (m^2 s^{-1}). Specifically, it is the ratio of the thermal conductivity k (W m^{-1} K^{-1}) to the volumetric heat capacity, which is the product of the mass density ρ (kg m^{-3}) and the specific heat capacity c (J K^{-1}) (Bergman et. al, 2011). However, if these physical properties are unknown then this prevents explicit calculation of the thermal diffusivity in this manner. This leads to the idea of

2

a laser flash experiment.

The laser flash method, first described in 1961, involves exposing the front surface of a thermally insulated material to a heat pulse of radiant energy for a short duration. The resulting temperature rise on the opposite, or rear, surface is then recorded (Parker et. al, 1961). It is the *half-rise time*, or time taken for the rear-surface temperature to reach half of its maximum value, that Parker et. al (1961) used as a key foundation for estimating the thermal diffusivity (Carr, 2019). In addition, Parker et. al (1961) made some simplifying assumptions, those being a homogeneous, thermally insulated sample, a heat pulse that is uniformly and instantaneously absorbed into a small portion of the sample, and unidirectional heat flow in one-dimensional geometries (Carr and Wood, 2019). Since the publication of research conducted by Parker et. al, the laser flash method has risen substantially in popularity (Vozár and Hohenauer, 2003).

Unsurprisingly, several modifications and advancements have been made to the method originally proposed by Parker et. al (1961). To elaborate, finite pulse time effects, heat losses, and accounting for high temperatures (Cowan, 1962) have been considered, in addition to extending the method to two-layer samples (Czél et. al, 2013). Recently, Carr (2019) proposed an alternate method for calculating the thermal diffusivity, under the same assumptions made by Parker et. al (1961). In this paper, Carr (2019) shows that the thermal diffusivity can be expressed in terms of the area enclosed by the rear-surface temperature rise curve and the steady state temperature (Baba, 2009). This new formula was found to be more robust, in relation to noisy data, than that proposed by Parker et. al (1961).

The foundation that Carr (2019) created was then extended upon shortly after. Specifically, the alternate expression for the thermal diffusivity was modified to accommodate, firstly, for finite pulse time effects only and then together with two-layered samples (Carr and Wood, 2019). However, it must be noted that the research described is limited to one-dimensional geometries. This report seeks to extend the work of Carr and Wood (2019) to radial, or unidirectional, heat diffusion in two- and three-dimensional annular and spherical shell geometries, respectively, as shown in Figure 1.
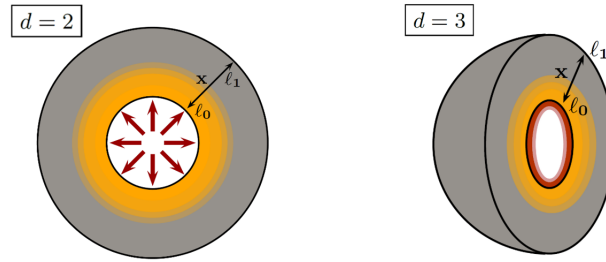
Figure 1: Radial heat diffusion in multi-dimensional geometries.

The application of a finite pulse time effect is considered on the interior boundary, followed by the external boundary, yielding one general formula with minor alterations in consideration of both cases. Numerical experiments are then conducted to mimic a realistic laser flash experiment, allowing the new formula for the thermal diffusivity to be rigorously tested. The same levels of noise used by Carr and Wood (2019) are employed, and it is found that the heat source location and number of dimensions strongly affect the accuracy of the new formula(s).

3   Statement of Authorship

The workload for this project was divided as follows:

- **Dr Elliot Carr** conceptualised the research project, guided the development of the mathematical results, supervised the research, assisted with implementation of code and interpretation of results, and reviewed this report.

- **Luke Filippini** developed the mathematical results, implemented code in MATLAB, performed numerical experiments, collated and interpreted the results, and wrote this report.

4   Mathematical Model

The mathematical model of key interest describes heat diffusion in the radial direction, defined as

$$\frac{\partial T}{\partial t} = \frac{\alpha}{x^{d-1}} \frac{\partial}{\partial x} \left(x^{d-1} \frac{\partial T}{\partial x} \right); \quad \ell_0 < x < \ell_1, \quad t > 0, \tag{1}$$

4

where $T(x,t)$ is the temperature (°C) of the sample at time t (s) and radial position x (m), d denotes the number of dimensions, and α represents the thermal diffusivity. Also, ℓ_0 and ℓ_1 denote the inner and outer boundaries, respectively.

For the derivation that follows, the initial condition

$$T(x,0) = 0 \tag{2}$$

is considered, accompanied by the boundary conditions

$$-k\frac{\partial T}{\partial x}(\ell_0, t) = q(t) \tag{3}$$

and

$$\frac{\partial T}{\partial x}(\ell_1, t) = 0, \tag{4}$$

where $q(t)$ represents a finite heat pulse applied uniformly at the inner surface $x = \ell_0$. Additionally, we define the amount of heat absorbed into the system at time t as $Q(t) = \int_0^t q(t)\ dt$. Given that the heat pulse is finite, it is assumed that the total amount of heat absorbed into the system, defined as $Q_\infty = \int_0^\infty q(t)\ dt$, is also finite. Moreover, any arbitrary heat pulse can be considered, provided that $\lim_{t\to\infty} q(t) = 0$. Lastly, because the heat pulse $q(t)$ is applied uniformly, the temperature at any given point is independent of the angular direction.

5 Steady State Derivation

5.1 General Solution

Derivation of new thermal diffusivity formulas, for two and three dimensions, requires expressions for the steady-state temperature. This is because the rear-surface integral, defined as $\int_0^\infty [T_\infty - T(\ell_1, t)]\ dt$ depends on a unique form of that temperature. To begin, let $T_\infty(x) = \lim_{t\to\infty} T(x,t)$ represent the steady-state temperature. Now, consider taking the limit as $t \to \infty$ of the radial heat diffusion model (1):

$$\lim_{t\to\infty}\left(\frac{\partial T}{\partial t}\right) = \lim_{t\to\infty}\left(\frac{\alpha}{x^{d-1}}\frac{\partial}{\partial x}\left(x^{d-1}\frac{\partial T}{\partial x}\right)\right).$$

5

By noting that $\frac{\partial T_\infty}{\partial t} = 0$, a homogeneous ODE is obtained for the steady state temperature T_∞,

$$\frac{\alpha}{x^{d-1}} \frac{d}{dx} \left(x^{d-1} \frac{dT_\infty}{dx} \right) = 0 \,. \tag{5}$$

The same limit can be taken over the boundary conditions (3) and (4). Noting that $\lim_{t \to \infty} q(t) = 0$, the boundary conditions for (5) become

$$T'_\infty (\ell_0) = T'_\infty (\ell_1) = 0 \,. \tag{6}$$

The ODE (5) can be integrated directly and rearranged to obtain

$$T'_\infty (x) = \frac{k_1}{x^{d-1}} \,,$$

an expression for the derivative of the steady-state temperature.

The only value of the arbitrary constant k_1 which satisfies condition (6) is $k_1 = 0$. Hence, the solution for the steady-state temperature must be a constant, defined here as $T_\infty = k_2$. An additional condition is required to determine a unique form of T_∞, namely conservation of energy. The law states that the change in heat in the sample must be balanced by the amount of heat entering the sample through the designated surface. From this point onwards, we consider the cases of two ($d = 2$) and three ($d = 3$) dimensions separately.

5.2   Two Dimensions

In two dimensions, conservation of energy is defined, in polar coordinates, as

$$\rho c \int_0^{2\pi} \int_{\ell_0}^{\ell_1} x \, T(x,t) \; dx \, d\theta = 2\pi \ell_0 Q(t) \,, \tag{7}$$

where $2\pi \ell_0$ is the circumference of the inner boundary. Taking the limit as $t \to \infty$, and integrating, allows the unique solution for T_∞, in two dimensions,

$$T_\infty = \frac{2\ell_0 Q_\infty}{\rho c \left(\ell_1^2 - \ell_0^2 \right)} \,, \tag{8}$$

to be determined.

5.3 Three Dimensions

The same process can be repeated in three dimensions. Conservation of energy, in spherical coordinates, is defined as

$$\rho c \int_0^\pi \int_0^{2\pi} \int_{\ell_0}^{\ell_1} x^2 \sin \varphi \, T(x,t) \, dx \, d\theta \, d\varphi = 4\pi \ell_0^2 Q(t) \tag{9}$$

where $4\pi \ell_0^2$ is the surface area of the inner sphere. Taking the limit as $t \to \infty$ and integrating yields

$$T_\infty = \frac{3\ell_0^2 Q_\infty}{\rho c \left(\ell_1^3 - \ell_0^3\right)} \tag{10}$$

as the unique solution for T_∞ in three dimensions.

5.4 General Formula

Finally, a general formula for the steady state temperature can be derived, simply by noting the forms of (8) and (10). The general form for the steady state temperature is

$$T_\infty = \frac{d\ell_0^{d-1} Q_\infty}{\rho c \left(\ell_1^d - \ell_0^d\right)}, \tag{11}$$

valid only for the radial heat diffusion model (1)–(4). The derivation of the steady-state temperature in the one-dimensional case, which (11) satisfies, can be found in Appendix 9.3.1.

6 Thermal Diffusivity Formulas

6.1 Derivation of ODE for $u(x)$

To begin deriving new thermal diffusivity formulas, consider the function below, which is a generalisation of the rear surface integral $\int_0^\infty \left[T_\infty - T(\ell_1,t)\right] dt$ to any position or location x,

$$u(x) = \int_0^\infty \left[T_\infty - T(x,t)\right] dt. \tag{12}$$

The primary objective is to determine an alternative form for $u(x)$, in both two and three dimensions, such that it can be equated to (12) and then evaluated at the rear surface $x = \ell_1$. Rearrangement for the thermal diffusivity α then follows. We start by defining the operator

$\mathcal{L} := \frac{\alpha}{x^{d-1}} \frac{\partial}{\partial x} \left(x^{d-1} \frac{\partial}{\partial x} \right)$ and applying it to (12). Carrying out the integral yields an ODE for $u(x)$,

$$\frac{\alpha}{x^{d-1}} \frac{d}{dx} \left(x^{d-1} \frac{du}{dx} \right) = -T_\infty. \tag{13}$$

Taking the derivative of (12) and evaluating at $x = \ell_0$, followed by $x = \ell_1$, gives two boundary conditions

$$u'(\ell_0) = \frac{Q_\infty}{k}, \quad u'(\ell_1) = 0, \tag{14}$$

analogous to (3) and (4).

6.2 Solving for $u(x)$

The ODE (13) can be rearranged and integrated directly to yield a general solution for the derivative,

$$u'(x) = -\frac{T_\infty}{d\alpha} x + \frac{a_1}{x^{d-1}}. \tag{15}$$

Incorporating both boundary conditions in (14) gives the same solution for the arbitrary constant a_1, that being $a_1 = \frac{T_\infty \ell_1^d}{d\alpha}$. This yields a unique solution for the derivative $u'(x)$,

$$u'(x) = \frac{T_\infty}{d\alpha} \left[\frac{\ell_1^d}{x^{d-1}} - x \right]. \tag{16}$$

6.2.1 Two Dimensions

The alternative form for $u(x)$ must now be solved for separately in two and three dimensions. We consider the case of two dimensions first. Firstly, the expression (16) is evaluated at $d = 2$ and integrated, providing a general solution for $u(x)$,

$$u(x) = a_0 + \frac{T_\infty}{2\alpha} \left[\ell_1^2 \ln x - \frac{1}{2} x^2 \right]. \tag{17}$$

To determine the arbitrary constant a_0, we need a condition akin to conservation of energy in two dimensions. By integrating (12) over the same limits as (7), multiplying through by x and the volumetric heat capacity ρc, and incorporating the steady state expression (8), such a condition is obtained:

$$\rho c \int_0^{2\pi} \int_{\ell_0}^{\ell_1} x u(x) \, dx \, d\theta = 2\pi \ell_0 \int_0^\infty [Q_\infty - Q(t)] \, dt. \tag{18}$$

8

Direct substitution of (17) into (18) yields a unique solution for a_0,

$$a_0 = \frac{2\ell_0 \int_0^\infty [Q_\infty - Q(t)] \ dt}{\rho c \left(\ell_1^2 - \ell_0^2\right)} - \frac{T_\infty}{4\alpha} \left[\frac{2\ell_1^2 \left(\ell_1^2 \ln \ell_1 - \ell_0^2 \ln \ell_0\right)}{\ell_1^2 - \ell_0^2} - \frac{1}{2}\left(3\ell_1^2 + \ell_0^2\right) \right],$$

implying that a unique solution for $u(x)$ in two dimensions is

$$u(x) = \frac{2\ell_0 \int_0^\infty [Q_\infty - Q(t)] \ dt}{\rho c \left(\ell_1^2 - \ell_0^2\right)} - \frac{T_\infty}{4\alpha} \left[x^2 - 2\ell_1^2 \ln x + \frac{2\ell_1^2 \left(\ell_1^2 \ln \ell_1 - \ell_0^2 \ln \ell_0\right)}{\ell_1^2 - \ell_0^2} - \frac{1}{2}\left(3\ell_1^2 + \ell_0^2\right) \right]. \quad (19)$$

6.2.2 Three Dimensions

Now, consider the expression (16) evaluated at $d = 3$. Direct integration provides a general solution for $u(x)$,

$$u(x) = b_0 - \frac{T_\infty}{3\alpha} \left[\frac{\ell_1^3}{x} + \frac{1}{2}x^2 \right]. \quad (20)$$

Again, an analogous condition to conservation of energy, in three dimensions, is required to determine a unique form of the arbitrary constant b_0. Following the same process as outlined in Section 6.2.1, a suitable condition is found to be

$$\rho c \int_0^\pi \int_0^{2\pi} \int_{\ell_0}^{\ell_1} x^2 \sin\varphi \, u(x) \ dx \ d\theta \ d\varphi = 4\pi\ell_0^2 \int_0^\infty [Q_\infty - Q(t)] \ dt. \quad (21)$$

Substituting (20) into (21) gives a unique solution for b_0,

$$b_0 = \frac{3\ell_0^2 \int_0^\infty [Q_\infty - Q(t)] \ dt}{\rho c \left(\ell_1^3 - \ell_0^3\right)} + \frac{T_\infty}{10\alpha} \left(\frac{6\ell_1^5 - \ell_0^2 \left(5\ell_1^3 + \ell_0^3\right)}{\ell_1^3 - \ell_0^3} \right),$$

which leads to a unique solution for $u(x)$,

$$u(x) = \frac{3\ell_0^2 \int_0^\infty [Q_\infty - Q(t)] \ dt}{\rho c \left(\ell_1^3 - \ell_0^3\right)} - \frac{T_\infty}{3\alpha} \left[\frac{\ell_1^3}{x} + \frac{1}{2}x^2 - \frac{18\ell_1^5 - 3\ell_0^2 \left(5\ell_1^3 + \ell_0^3\right)}{10\left(\ell_1^3 - \ell_0^3\right)} \right]. \quad (22)$$

6.3 Determining Thermal Diffusivity

Finally, equating (19) and (22) to (12) leads to formulas for the thermal diffusivity in two and three dimensions, respectively. Considering the two-dimensional case, equating (19) and (12), evaluating the equation at $x = \ell_1$, and rearranging for α yields a formula for the thermal diffusivity,

$$\alpha = \frac{1}{8\left(I_T - I_q\right)} \left[\frac{\ell_1^4 + 4\ell_1^2 \ell_0^2 \int_{\ell_1}^{\ell_0} \frac{1}{x} \, dx - \ell_0^4}{\ell_1^2 - \ell_0^2} \right]. \quad (23)$$

Performing the same process in the three-dimensional case gives the formula

$$\alpha = \frac{1}{10\left(I_T - I_q\right)} \left[\frac{\ell_1^5 + 5\ell_1^3\ell_0^3 \int_{\ell_1}^{\ell_0} \frac{1}{x^2}\, dx - \ell_0^5}{\ell_1^3 - \ell_0^3}\right], \tag{24}$$

where I_T and I_q are defined as

$$I_T = \int_0^\infty \left[1 - \frac{T\left(\ell_1, t\right)}{T_\infty}\right]\, dt \quad I_q = \int_0^\infty \left[1 - \frac{Q\left(t\right)}{Q_\infty}\right]\, dt$$

6.3.1   General Formula

In the one-dimensional case, the formula in Appendix 9.3.2 can be manipulated into the form

$$\alpha = \frac{1}{6\left(I_T - I_q\right)} \left[\frac{\ell_1^3 + 3\ell_1\ell_0 \int_{\ell_1}^{\ell_0} dx - \ell_0^3}{\ell_1 - \ell_0}\right]. \tag{25}$$

Hence, it is entirely reasonable, based off the similar forms of (23), (24), and (25), to suggest that a general form for the thermal diffusivity is

$$\alpha = \frac{1}{2\left(d + 2\right)\left(I_T - I_q\right)} \left[\frac{\ell_1^{d+2} + \left(d + 2\right)\ell_1^d\ell_0^d \int_{\ell_1}^{\ell_0} \frac{1}{x^{d-1}}\, dx - \ell_0^{d+2}}{\ell_1^d - \ell_0^d}\right], \tag{26}$$

valid only for the radial heat diffusion model (1)–(4).

6.4   Application of Heat Source on Outer Surface

A natural question that arises is how applying the finite heat pulse to the outer boundary alters the analysis previously carried out. Suppose the boundary conditions of the model (1)–(4) are swapped to accommodate for this change,

$$\frac{\partial T}{\partial x}\left(\ell_0, t\right) = 0, \quad \frac{\partial T}{\partial x}\left(\ell_1, t\right) = \frac{q\left(t\right)}{k}. \tag{27}$$

For brevity, it turns out that applying the same processes in Sections 5 and 6 yields a formula visually identical to (26), with minor differences occurring in the definition of the integral I_T and the steady state temperature T_∞,

$$I_T = \int_0^\infty \left[1 - \frac{T\left(\ell_0, t\right)}{T_\infty}\right]\, dt, \quad T_\infty = \frac{d\ell_1^{d-1}Q_\infty}{\rho c\left(\ell_1^d - \ell_0^d\right)}.$$

7 Discussion and Results

7.1 Synthetic Data Using Finite Volume Method

The thermal diffusivity formula (26) can be verified using synthetic data, representing the rear-surface temperature rise. To elaborate, the model (1)–(4), and also with alternate boundary conditions (27), can be solved numerically using the *finite volume method*. This method converts a spatially-continuous initial-boundary value problem into a spatially-discrete initial-value problem. Hence, the temperature rise can be well approximated at a suitable number of points in both space and time.

Let N denote the number of spatial nodes at which the solution $T(x,t)$ is to be approximated. These nodes are labelled $x_1, ..., x_N$, and the corresponding numerical approximations are labelled $T_1, ..., T_N$, where $T_i \approx T(x_i, t)$, for $i = 1, ..., N$. The nodes are defined such that $x_1 = \ell_0$ and $x_N = \ell_1$. Following on, let $V_i = e_i - w_i$ denote the control volume for the ith node, where

$$e_i = \begin{cases} \frac{x_{i+1}+x_i}{2}, & i = 1, \ldots, N-1 \\ x_N, & i = N \end{cases} \quad \text{and} \quad w_i = \begin{cases} \frac{x_i+x_{i-1}}{2}, & i = 2, \ldots, N \\ x_1, & i = 1 \end{cases}$$

are the west and east control volume boundaries, respectively. Lastly, let $h_i = x_{i+1} - x_i$ denote the spacing between each of the nodes.

Integrating (1) over each control volume interval $[w_i, e_i]$, for $i = 1, \ldots, N$, and applying boundary conditions (3)–(4) yields a set of N ODEs). For an internal heat source, the ODEs are

$$\frac{dT_1}{dt} = \frac{\alpha}{V_1 \ell_0^{d-1}} \left[-\frac{e_1^{d-1}}{h_1} T_1 + \frac{e_1^{d-1}}{h_1} T_2 + \frac{\ell_0^{d-1} q(t)}{k} \right],$$

$$\frac{dT_i}{dt} = \frac{\alpha}{V_i x_i^{d-1}} \left[\frac{w_i^{d-1}}{h_{i-1}} T_{i-1} - \left(\frac{w_i^{d-1}}{h_{i-1}} + \frac{e_i^{d-1}}{h_i} \right) T_i + \frac{e_i^{d-1}}{h_i} T_{i+1} \right], \quad (i = 2, ...N-1)$$

$$\frac{dT_N}{dt} = \frac{\alpha}{V_N \ell_1^{d-1}} \left[\frac{w_N^{d-1}}{h_{N-1}} T_{N-1} - \frac{w_N^{d-1}}{h_{N-1}} T_N \right].$$

11

Alternatively, incorporating an outer heat source, with boundary conditions (27), alters the first and last ODEs, giving

$$\frac{dT_1}{dt} = \frac{\alpha}{V_1 \ell_0^{d-1}} \left[-\frac{e_1^{d-1}}{h_1} T_1 + \frac{e_1^{d-1}}{h_1} T_2 \right], \quad \frac{dT_N}{dt} = \frac{\alpha}{V_N \ell_1^{d-1}} \left[\frac{w_N^{d-1}}{h_{N-1}} T_{N-1} - \frac{w_N^{d-1}}{h_{N-1}} T_N + \frac{\ell_1^{d-1} q(t)}{k} \right].$$

The above set of ODEs, for either an internal or external heat source, are then solved using MATLAB's **ode15s** solver, using absolute and relative error tolerances of 10^{-12}. Very accurate approximations are obtained for the temperature at specific points in space and time. Figure 2 provides an example of synthetic data for the rear-surface temperature rise, accounting for both heat source locations.

(a) Inner Heat Source   (b) Outer Heat Source
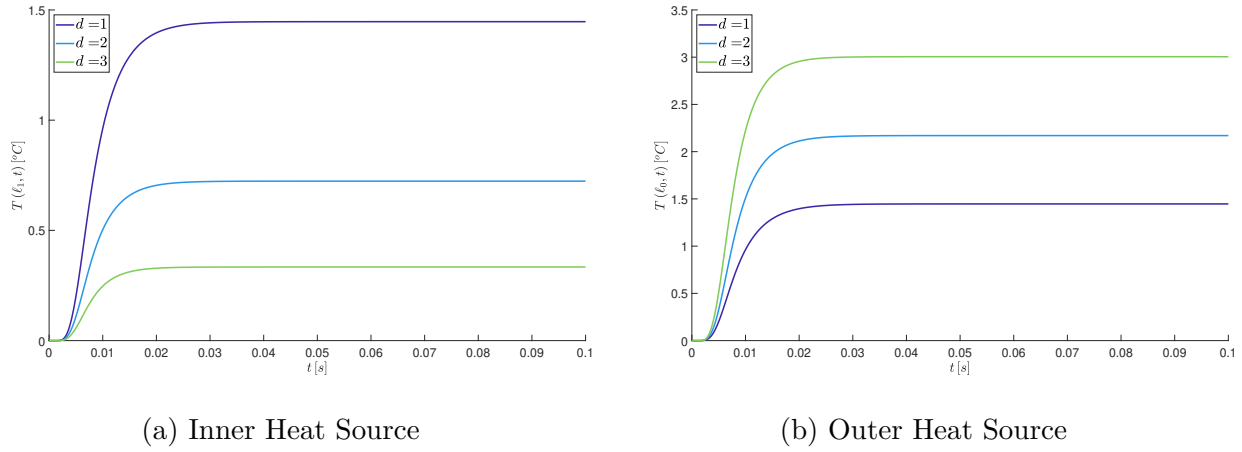
Figure 2: Synthetic Rear Surface Temperature Rise Curves.

For this numerical experiment, and those that follow, a triangular heat pulse was used, with finite pulse time $\tau = 0.005$ seconds and pulse peak occurring at $\beta = 0.001$ seconds.

$$q(t) = \begin{cases} \frac{2Q_\infty t}{\tau \beta}, & 0 < t \le \beta \\ \frac{2Q_\infty(\tau - t)}{\tau(\tau - \beta)}, & \beta \le t \le \tau \\ 0, & \text{otherwise} \end{cases} \tag{28}$$

To generate the synthetic data, the following parameter values were used: $k = 222$ W m^{-1} K^{-1}, $\rho = 2700$ kg m^{-3}, $c = 896$ J K^{-1}, giving a target value of $\alpha = 9.1766 \times 10^{-5}$ m^2 s^{-1} for the thermal diffusivity. Additionally, radial boundaries of $\ell_0 = 0.001$ (m) and $\ell_1 = 0.003$ (m), an end time of $t_N = 0.1$ (s), $N = 501$ spatial nodes, and a temporal spacing of $\delta t = 10^{-4}$ were

chosen. These parameter values are consistent with those used by Carr and Wood (2019) and are used in the analysis that follows.

Finally, the trapezoidal rule is used to calculate an approximation to the integral I_T. Let $T_r(t_j)$ be the numerical approximation of the rear-surface temperature rise at time $t = t_j$, for $j = 1, \ldots, M+1$, where M is the number of temporal spacings. Thus, direct substitution of the approximation

$$I_T \approx \frac{\delta t}{2}\left[T_1^* + 2\sum_{i=2}^{M} T_i^* + T_{M+1}\right], \quad \text{where} \quad T_j^* = 1 - \frac{T_r(t_j)}{T_\infty},$$

into (26) yields highly accurate estimates for the thermal diffusivity. The results are the same for both heat source locations.

Target Value: $\alpha = 9.1766 \times 10^{-5}$

$d = 1$	$d = 2$	$d = 3$
9.1766×10^{-5}	9.1766×10^{-5}	9.1765×10^{-5}

Table 1: Estimates of α using synthetic data.

7.2   Verification Using Noisy Data

Carr and Wood (2019) have already shown that the rear-surface integral method, incorporating a finite pulse time effect, is less sensitive to measurement error (noisy data) than the half-rise time method originally proposed by Parker et. al (1961). Thus, the analysis below investigates how a change in both the number of dimensions and the boundary at which heat is applied affects the accuracy of the general formula (26). For all tests, the same three levels of noise are used, to be consistent with previous work.

We consider the case of adding Gaussian noise to the rear-surface temperature rise to mimic a realistic laser flash experiment. This is defined mathematically as

$$\tilde{T}_i = T_r(t_i) + z_i, \quad \text{for} \quad i = 1, ..., N,$$

where z_i is a random sample drawn from a normal distribution with mean zero and standard deviation σ. The numerical experiments conducted use low ($\sigma = 0.005$), moderate ($\sigma = 0.02$)

and high ($\sigma = 0.05$) levels of noise (Carr and Wood, 2019).

For one trial, an estimate of the thermal diffusivity, denoted as $\tilde{\alpha}$, is calculated using the rear-surface temperature rise with added noise. The relative error as a percentage, $\varepsilon = \frac{\tilde{\alpha} - \alpha}{\alpha} \times 100\%$, is then determined to gauge the accuracy of the estimate. Over 10,000 realisations, we can construct histograms for both the percentage error and thermal diffusivity estimates, which provide valuable insight into the overall trends and accuracy of the general formula (26).

Figure 3, in Appendix 9.1, assumes that a heat source is applied on the internal boundary. Clearly, an increasing number of dimensions is associated with a rear-surface temperature rise of reduced significance. As expected, the histograms depict a wider range for both the percentage error and thermal diffusivity estimates as the noise level increases. However, they also show that numerical estimation of the integral I_T, using the trapezoidal rule, becomes less reliable as the temperature rise decreases in significance. Hence, this affects the accuracy of the thermal diffusivity formula (26).

The histogram statistics gathered from the tests displayed in Figure 3 are provided in Table 2. As the number of dimensions increases, the absolute value of the mean, the standard deviation, and gap between the minimum and maximum values of the percentage error also tend to increase. This trend is far more bold and noticeable as the noise level rises. These effects are clearly noticeable in the last three columns of Table 2. To elaborate, the accuracy of the mean thermal diffusivity, in relation to the target value of $\alpha = 9.1766 \times 10^{-5}$, decreases as the number of dimensions increases, which is again amplified by the level of noise. The minimum and maximum values stray further from the true value due to the same cause.

In Appendix 9.2, Figure 4 and Table 3 display the results of applying the heat source to the exterior boundary and conducting identical numerical experiments. The result is an opposite effect to that described immediately above; namely, that that sensitivity of the thermal diffusivity formula (26) to measurement error decrease with the number of the dimensions. This

is because the rear-surface temperature rise curve is more prominent with an increasing number of dimensions.

8   Conclusion

In this report, an extension to the rear-surface integral method, with finite pulse time effects, has been provided (Carr and Wood, 2019). Specifically, the method has been extended to investigate heat diffusion in the radial direction for two- and three-dimensional annual and spherical geometries, respectively. By extending the rear-surface integral method developed by Carr (2019), a general formula for the thermal diffusivity, applicable to any dimension, was derived. It must be stated that the formula differs slightly depending on the location of the heat source, and it is only valid for the model (1)–(4), or that with boundary conditions (27).

The new formula(s) for the thermal diffusivity was tested by adding Gaussian noise to an accurate numerical solution of the rear-surface temperature rise for 10,000 realisations. It was found that as the temperature rise curves, and corresponding steady-state temperatures, lowered in magnitude, estimations of the thermal diffusivity exhibited larger variability and, hence, a decrease in accuracy.

This work has only extended on the finite pulse time effect introduced by Carr and Wood (2019). Hence, further work could be done to investigate radial heat flow in two-layer samples. Additionally, the effects of measurement noise were only considered for three fixed levels of noise. Thus, another possible extension would be to investigate how scaling the noise levels with a change in the number of dimensions affects the results.

9 Appendix

9.1 Noise Experiments with an Inner Heat Source
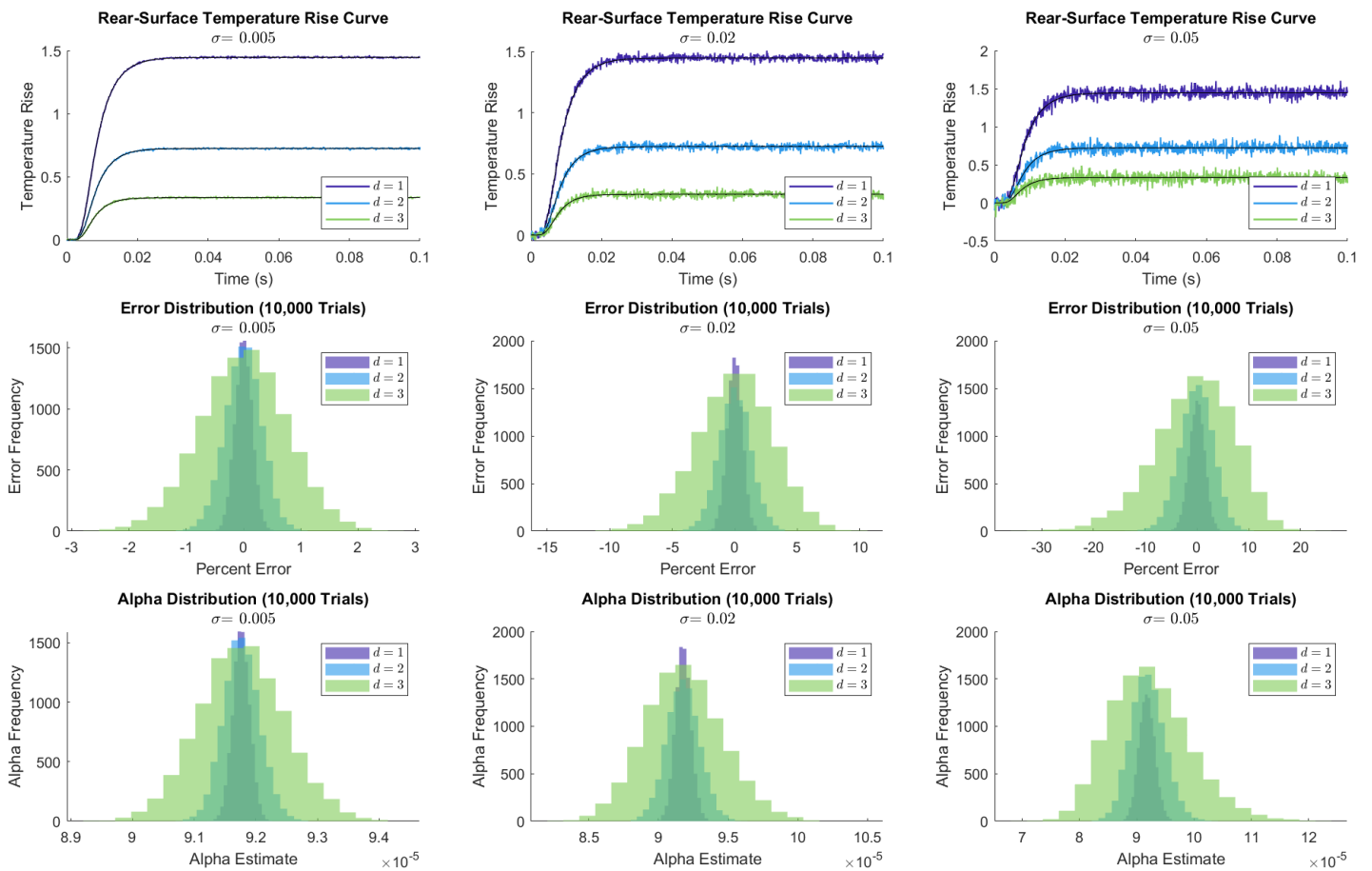
Figure 3: Effects of various noise levels over 10,000 realisations (inner heat source).

Dimension	$\sigma(z)$	$\mu(\varepsilon)$	$\sigma(\varepsilon)$	$\min(\varepsilon)$	$\max(\varepsilon)$	$\mu(\tilde{\alpha})$	$\min(\tilde{\alpha})$	$\max(\tilde{\alpha})$
	0.005	0.0021	0.1499	-0.5834	0.5704	9.1764×10^{-5}	9.1242×10^{-5}	9.2301×10^{-5}
$d=1$	0.02	-0.0012	0.6015	-2.8750	2.5509	9.1769×10^{-5}	8.9425×10^{-5}	9.4404×10^{-5}
	0.05	-0.0225	1.5050	-5.1536	4.8764	9.1787×10^{-5}	8.7291×10^{-5}	9.6495×10^{-5}
	0.005	-0.0022	0.3149	-1.2851	1.1087	9.1768×10^{-5}	9.0748×10^{-5}	9.2945×10^{-5}
$d=2$	0.02	-0.0012	1.2777	-5.3311	3.9913	9.1767×10^{-5}	8.8103×10^{-5}	9.6658×10^{-5}
	0.05	-0.1255	3.2020	-13.5323	10.8871	9.1881×10^{-5}	8.1775×10^{-5}	1.0418×10^{-4}
	0.005	-0.0043	0.7494	-2.7077	2.6390	9.1770×10^{-5}	8.9344×10^{-5}	9.4251×10^{-5}
$d=3$	0.02	-0.0469	3.0183	-14.2802	10.4459	9.1809×10^{-5}	8.2180×10^{-5}	1.0487×10^{-4}
	0.05	-0.5548	7.5835	-34.6505	24.9569	9.2275×10^{-5}	6.8864×10^{-5}	1.2356×10^{-4}

Table 2: Key statistics from noise experiments (inner heat source).

9.2 Noise Experiments with an Outer Heat Source
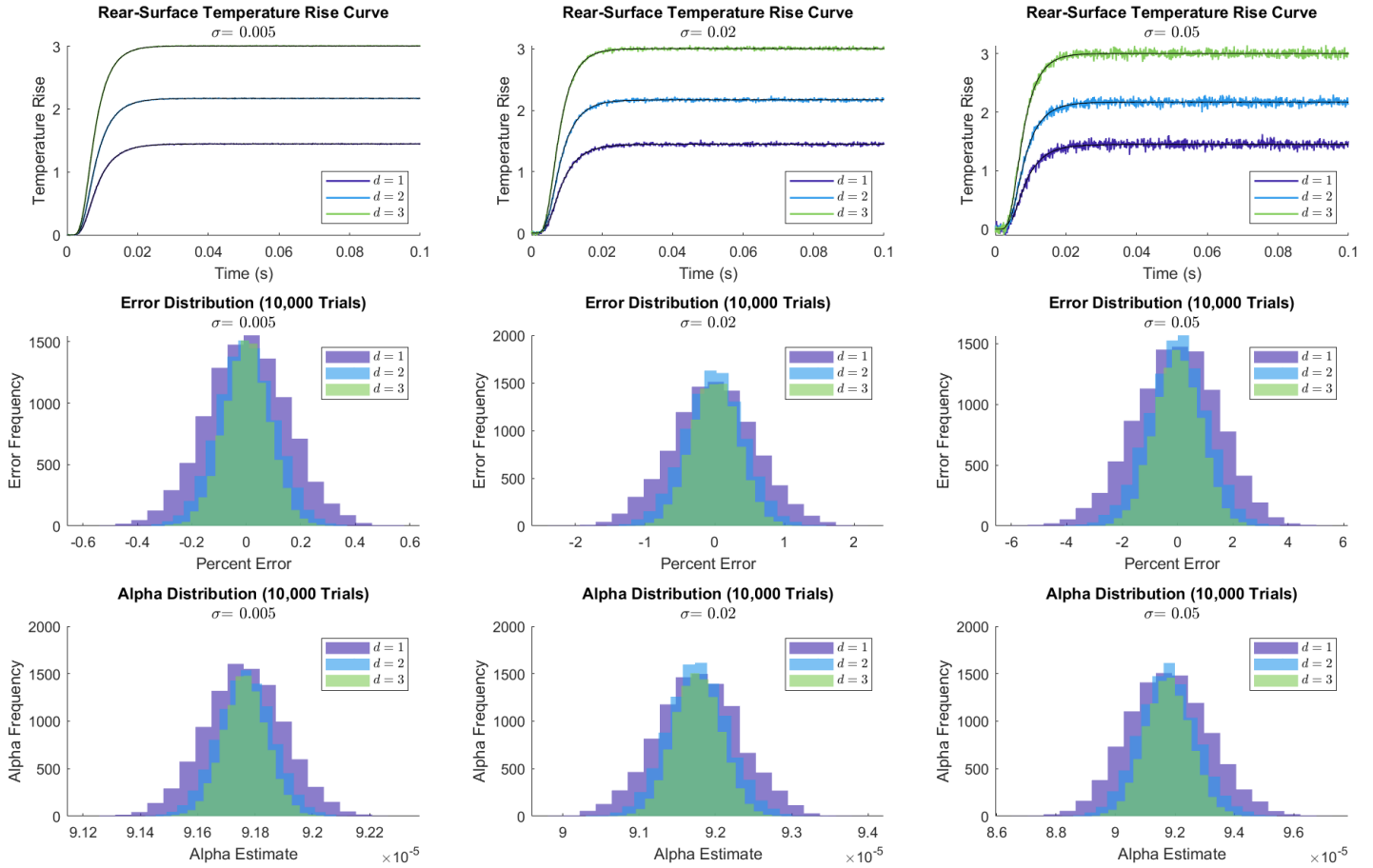
Figure 4: Effects of various noise levels over 10,000 realisations (outer heat source).

Dimension	$\sigma(z)$	$\mu(\varepsilon)$	$\sigma(\varepsilon)$	$\min(\varepsilon)$	$\max(\varepsilon)$	$\mu(\tilde{\alpha})$	$\min(\tilde{\alpha})$	$\max(\tilde{\alpha})$
	0.005	0.0034	0.1496	-0.5949	0.5626	9.1763×10^{-5}	9.1250×10^{-5}	9.2312×10^{-5}
$d=1$	0.02	-0.0127	0.5963	-2.2751	2.1313	9.1777×10^{-5}	8.9810×10^{-5}	9.3854×10^{-5}
	0.05	-0.0287	1.4940	-5.8266	5.5457	9.1792×10^{-5}	8.6677×10^{-5}	9.7113×10^{-5}
	0.005	1.5297×10^{-5}	0.1048	-0.3648	0.4013	9.1766×10^{-5}	9.1398×10^{-5}	9.2101×10^{-5}
$d=2$	0.02	-0.0026	0.4254	-1.8659	1.5931	9.1768×10^{-5}	9.0304×10^{-5}	9.3478×10^{-5}
	0.05	-0.0095	1.0591	-4.2806	3.6489	9.1775×10^{-5}	8.8417×10^{-5}	9.5694×10^{-5}
	0.005	6.9599×10^{-4}	0.0825	-0.2919	0.3012	9.1765×10^{-5}	9.1489×10^{-5}	9.2034×10^{-5}
$d=3$	0.02	0.0018	0.3316	-1.3155	1.2268	9.1764×10^{-5}	9.0640×10^{-5}	9.2973×10^{-5}
	0.05	-0.0017	0.8240	-3.1732	2.6755	9.1767×10^{-5}	8.9311×10^{-5}	9.4678×10^{-5}

Table 3: Key statistics from noise experiments (outer heat source).

9.3 Derivations in the One-Dimensional Case

9.3.1 Steady-State Temperature

Using the results of Section 5.1, we continue from the point where the steady state temperature is shown to be a constant for all dimensions, $T_\infty = k_2$. To determine the form of the steady state temperature, the law of conservation of energy in one dimension is considered.

$$\rho c \int_{\ell_0}^{\ell_1} T(x,t) \ dx = Q(t) \tag{29}$$

That is, the change in heat in the interval $[\ell_0, \ell_1]$ must be balanced by the amount of heat entering through the front surface. Taking the limit as $t \to \infty$,

$$\lim_{t\to\infty} \left(\rho c \int_{\ell_0}^{\ell_1} T(x,t) \ dx \right) = \lim_{t\to\infty} Q(t) \,,$$

yields a formula for the steady state temperature,

$$T_\infty = \frac{Q_\infty}{\rho c (\ell_1 - \ell_0)} \,.$$

9.3.2 Thermal Diffusivity

Consider equation (15), defined as

$$u'(x) = \frac{T_\infty}{\alpha d} \left[\frac{\ell_1^d}{x^{d-1}} - x \right],$$

for ease of reference. In one dimension, the derivative can be simplified and integrated to determine a general form for $u(x)$,

$$u(x) = c_0 + \frac{T_\infty}{\alpha} \left[\ell_1 x - \frac{1}{2} x^2 \right]. \tag{30}$$

To determine the form of c_0, there needs to be an analogous condition to conservation of energy in one dimension. The condition can be determined by integrating (12) over the interval $[\ell_0, \ell_1]$ and multiplying by the volumetric heat capacity ρc, giving

$$\rho c \int_{\ell_0}^{\ell_1} u(x) \ dx = \rho c \int_0^\infty \int_{\ell_0}^{\ell_1} [T_\infty - T(x,t)] \ dx \ dt,$$

which, after incorporating (29), ultimately yields

$$\rho c \int_{\ell_0}^{\ell_1} u(x) \ dx = \int_0^\infty [Q_\infty - Q(t)] \ dt. \tag{31}$$

Thus, substituting (30) into (31) yields

$$c_0 = \frac{\int_0^\infty [Q_\infty - Q(t)] \ dt}{\rho c (\ell_1 - \ell_0)} - \frac{T_\infty}{6\alpha} \left[\frac{2\ell_1^3 - 3\ell_1 \ell_0^2 + \ell_0^3}{\ell_1 - \ell_0} \right]$$

as the solution for c_0, implying that the solution for $u(x)$ in the one-dimensional case is

$$u(x) = \frac{\int_0^\infty [Q_\infty - Q(t)] \ dt}{\rho c (\ell_1 - \ell_0)} + \frac{T_\infty}{\alpha} \left[\ell_1 x - \frac{1}{2} x^2 - \frac{2\ell_1^3 - 3\ell_1 \ell_0^2 + \ell_0^3}{6(\ell_1 - \ell_0)} \right]. \tag{32}$$

Finally, equating (12) and (32), both evaluated at $x = \ell_1$, yields a formula for the thermal diffusivity α,

$$\alpha = \frac{(\ell_1 - \ell_0)^2}{6(I_T - I_q)}.$$

10   Bibliography

1. Baba, T., 2009, 'Analysis of one-dimensional heat diffusion after light pulse heating by the response function method', *Japanese Journal of Applied Physics*, vol. 48, no. 5S2, p. 05EB04

2. Bergman, T.L., Lavine, A.S., Incropera, F.P. & Dewitt, D.P., 2011, *Fundamentals of Heat and Mass Transfer*, 7th edn., John Wiley & Sons Inc., Hoboken, NJ

3. Carr, E.J., 2019, 'Rear-surface integral method for calculating thermal diffusivity from laser flash experiments', *Chemical Engineering Science*, vol. 199, pp. 546–551

4. Carr, E.J., & Wood, C.J., 2019, 'Rear-surface integral method for calculating thermal diffusivity: Finite pulse time correction and two-layer samples', *International Journal of Heat and Mass Transfer*, vol. 144, p. 118609

5. Cowan, R.D., 1962, 'Pulse method of measuring thermal diffusivity at high temperatures', *Journal of Applied Physics*, vol. 34, no. 4, pp. 926–927

6. Czél, B., Woodbury, K.A., & Gróf, G., 2013, 'Analysis of parameter estimation possibilities of the thermal contact resistance using the laser flash method with two-layer specimens', *International Journal of Thermophysics*, vol. 34, no. 10, pp. 1993–2008

7. Parker, W.J., Jenkins, R.J., Butler, C.P. & Abbott, G.L., 1961, 'Flash method of determining thermal diffusivity, heat capacity, and thermal conductivity', *Journal of Applied Physics*, vol. 32, no. 9, pp. 1679–1684

8. Salazar, A., 2003, 'On thermal diffusivity', *European Journal of Physics*, vol. 24, no. 4, pp. 351–358

9. Vozár, L., & Hohenauer, W., 2003, 'Flash method of measuring the thermal diffusivity. A review.', *High Temperatures - High Pressures*, vol. 36, no. 3, pp. 253–264